REPORT DOCUMENTATION PAGE

1a. REPORT SECURITY CLASSIFICATION UNCLASSIFIED	1b. RESTRICTIVE MARKINGS

2a. SECURITY CLASSIFICATION AUTHORITY	3. DISTRIBUTION/AVAILABILITY OF REPORT
2b. DECLASSIFICATION/DOWNGRADING SCHEDULE	Approved for public release; distribution is unlimited

4. PERFORMING ORGANIZATION REPORT NUMBER(S)	5. MONITORING ORGANIZATION REPORT NUMBER(S)

6a. NAME OF PERFORMING ORGANIZATION Mech. Engineering Dept. Naval Postgraduate School	6b. OFFICE SYMBOL (if applicable) ME	7a. NAME OF MONITORING ORGANIZATION Naval Postgraduate School

6c. ADDRESS (City, State, and ZIP Code) Monterey, CA 93943-5000	7b. ADDRESS (City, State, and ZIP Code) Monterey, CA 93943-5000

8a. NAME OF FUNDING/SPONSORING ORGANIZATION	8b. OFFICE SYMBOL (if applicable)	9. PROCUREMENT INSTRUMENT IDENTIFICATION NUMBER

8c. ADDRESS (City, State, and ZIP Code)	10. SOURCE OF FUNDING NUMBERS			
	PROGRAM ELEMENT NO.	PROJECT NO.	TASK NO.	WORK UNIT ACCESSION NO.

11. TITLE (Include Security Classification)
CONTINUOUS MEASUREMENT BY EDDY CURRENT METHODS OF AGE HARDENING IN AN ALUMINUM ALLOY, UNC.

12. PERSONAL AUTHOR(S)
Esarey, John G.

13a. TYPE OF REPORT Master's Thesis	13b. TIME COVERED FROM 04/92 TO: 09/92	14. DATE OF REPORT (Year, Month, Day) 1992, SEPTEMBER	15. PAGE COUNT 47

16. SUPPLEMENTARY NOTATION The views expressed in this thesis are those of the author and do not reflect the official policy or position of the Department of Defense or the United States Government.

17.	COSATI CODES		18. SUBJECT TERMS (Continue on reverse if necessary and identify by block number)
FIELD	GROUP	SUB-GROUP	Eddy Current Monitoring, Resistivity Measurement, Age Hardening, Precipitation Hardening

19. ABSTRACT (Continue on reverse if necessary and identify by block number)

   Many materials processing operations such as age hardening heat treatments typically involve following predetermined time and temperature schedules to obtain the desired final material properties. The intelligent processing approach is to develop sensors for monitoring of material response to processing operations in real time. As an alloy age hardens its electrical resistivity changes. Hence, the process of aging can be monitored by measuring the change in resistivity relative to that of a non-age hardening material such as fully annealed pure aluminum. A device using two small, spiral-wound probes was designed and used to induce eddy currents within the pure aluminum and the aging alloy. The probes were incorporated as elements in an impedance bridge circuit. The bridge unbalance voltage decreased in value over time indicating decreasing resistivity during the aging process. The monitoring concept was verified. Refinements such as improved impedance bridge circuitry and probe size/test frequency optimization are needed to unlock its full potential.

20. DISTRIBUTION/AVAILABILITY OF ABSTRACT [X] UNCLASSIFIED/UNLIMITED ☐ SAME AS RPT. ☐ DTIC USERS	21. ABSTRACT SECURITY CLASSIFICATION UNCLASSIFIED	
22a. NAME OF RESPONSIBLE INDIVIDUAL T.R McNelley	22b. TELEPHONE (Include Area Code) (408) 646-2589	22c. OFFICE SYMBOL ME/MC

DD FORM 1473, 84 MAR	83 APR edition may be used until exhausted All other editions are obsolete	SECURITY CLASSIFICATION OF THIS PAGE UNCLASSIFIED

T259146

Continuous Measurement By Eddy Current Methods
of Age Hardening in Aluminum Alloys

by

John Gilbert Esarey
Lieutenant, United States Navy
B.S.M.E.T., University of Southern Indiana, 1985

Submitted in partial fulfillment of the
requirements for the degree of

MASTER OF SCIENCE IN MECHANICAL ENGINEERING

from the

NAVAL POSTGRADUATE SCHOOL
September, 1992

ABSTRACT

Many materials processing operations such as age hardening heat treatments typically involve following predetermined time and temperature schedules to obtain the desired final material properties. The intelligent processing approach is to develop sensors for monitoring of material response to processing operations in real time. As an alloy age hardens its electrical resistivity changes. Hence, the process of aging can be monitored by measuring the change in resistivity relative to that of a non-age hardening material such as fully annealed pure aluminum. A device using two small, spiral-wound probes was designed and used to induce eddy currents within the pure aluminum and the aging alloy. The probes were incorporated as elements in an impedance bridge circuit. The bridge unbalance voltage decreased in value over time indicating decreasing resistivity during the aging process. The monitoring concept was verified. Refinements such as improved impedance bridge circuitry and probe size/test frequency optimization are needed to unlock its full potential.

TABLE OF CONTENTS

LIST OF FIGURES

ACKNOWLEDGEMENTS

A special thanks to my thesis advisor, Professor Terry McNelley, who allowed me to take the risk/opportunity to break new ground in the area of intelligent processing. The Esarey - McNelley measuring process was designed due to Prof. McNelley having the insight to ask the right question. Answering his question, "Do you think you could come up with a way to monitor resistivity changes in an age hardening aluminum alloy at temperature using a non-intrusive method such as an eddy current device?", shall be a memory which will never fade.

I am especially grateful to Mr. John Flarity of Flare Technologies for his excellent technical advice as well as his generosity in supplying me with small hardware items, saving myself and the U.S. Navy time and money. Mr. Flarity's good nature and wealth of technical knowledge were critical ingredients to sustaining my sanity during the course of this research effort.

The unwavering technical support received form Tom Christian and the Naval Postgraduate School machine shop was second to none and very much appreciated.

The Naval Air Warfare Center's support, with Dr. William Frazer as program monitor, in developing the intelligent processing concept, is acknowledged and much appreciated.

For the most important people in my life, my family, without whom I certainly would not be where I am today. Thanks for all the encouragement, love, and support, especially from my wife Patti. I only wish that I had been able to spend more time with you. And finally, a special thank you to my sons and daughter, Justin, Samuel and Brooke for making me smile even when my mind was pre-occupied.

I. INTRODUCTION

The primary focus of this thesis project was to design, fabricate and test a simple eddy current sensor device which could be used to monitor in real time the isothermal age hardening of aluminum alloys. The age hardening of aluminum alloys has been accomplished primarily by the development of empirical time at temperature data correlated to mechanical, electrical, corrosion and various other properties. This practice of applying a standard heat treatment schedule to achieve a designated age hardened condition does not provide any indication of the progress, success or failure of the age hardening process in real time. Only upon completion of the aging treatment is the success or failure of the age hardening process measured by destructive or non-destructive methods. A wide range of methods may be employed, including resistivity testing by eddy current methods. At present, resistivity testing with eddy current devices to determine the extent of aging in aluminum alloys is conducted at near room temperatures and is a post-heat treatment measurement.

Monitoring the process in real time utilizing a computerized control system would allow the heat treatment process to be terminated when the desired properties are obtained as opposed to an after-the-fact determination of success or failure. The concept of process monitoring and control in real time is known as intelligent processing. An eddy current sensing device linked to the computerized control system mentioned above would establish an intelligent approach to age hardening of aluminum alloys. With this goal in mind the concept of utilizing existing eddy current resistivity measuring equipment was first considered. As mentioned above, existing resistivity measuring devices are primarily used to obtain an indication of a material's resistivity essentially at room temperature with a temperature correction factor being applied to allow for small deviations from the calibration temperature.

Such devices normally give output values in absolute units such as $\Omega \times cm$ or percent of the international annealed copper standard (%IACS) and can be quite accurate. Utilizing a high temperature probe, one could possibly modify such a device to monitor the age hardening process. However, conversion cost and calibration could become considerable obstacles. The relatively complex and tedious task of obtaining accurate absolute numerical resistivity values, even near room temperature, sparked the desire to achieve the goal with a less complex system. A monitoring technique was devised based on the premise that sensing relative resistivity changes during aging versus obtaining absolute resistivity values was all that was needed to accurately reflect the aging process. One should note that this premise relies on the assumption that solutionizing of the material to be aged was performed properly and consistently. However, it is feasible to include a computer subroutine to notify the operator of starting conditions which are inconsistent with those expected for the particular alloy being aged at the specified aging temperature. The system designed and tested during this period of research basically consisted of the following five components:

1) Two spiral-wound sensor probes mounted in a testing apparatus;
2) An impedance bridge circuit;
3) An Interstate Electronics Corp. F36 Function Generator;
4) A Hewlett Packard 3478A Digital Multimeter with an HP-IB interface bus;
5) A Hewlett Packard PC (with IEEE 488 data acquisition board installed) to collect time and voltage data for subsequent analysis.

Utilizing the above equipment, time and impedance bridge unbalance (r.m.s.) voltage data files which were obtained. Plots of aging time vs. mV as well as aging time vs. percent deviation from (mean) peak impedance bridge output were generated for various time/temperature aging conditions. These plots revealed clear decreases in resistivity during the aging process for all time/temperature aging conditions. More importantly, the rate of decrease in resistivity increased as the

2

aging temperature increased. These results were consistent with known trends in resistivity for age-hardenable alloys thereby verifying the monitoring concept.

II. BACKGROUND

A. ELECTRICAL RESISTIVITY

A basic knowledge of the factors governing the electrical resistivity of aluminum and its alloys is necessary to understand fully how eddy current probe coils interact with the tested samples. A detailed development of the electrical behavior of metals is presented in References 1 and 2. The current work involves the exploitation of the change in electrical resistivity of age hardenable aluminum alloys during aging and requires a repeatable reference condition. Aluminum alloys are metallically bonded materials and their resistivities is governed primarily by the ease with which valance electrons (charge carriers) can move within the material. The ease with which these charge carriers can move is commonly defined as mobility $(\mu, cm^2/(V \cdot sec))$. The resistivity, ρ, of a material is given by the relation:

$$\rho = \frac{1}{nq\mu} \quad \Omega \cdot cm \text{ (Eq 2.1)}$$

where n is the number of charge carriers, q is the carrier charge and μ is their mobility. The charge, q, on each carrier is a constant value of 1.6×10^{-19} Coulombs and n is approximately constant for the alloys tested. This leaves resistivity, ρ, as a function of mobility, μ. For the materials considered in this work the mobility, μ, depends on lattice imperfections, microstructure, and temperature. An example calculation for the theoretical mobility, μ, of pure aluminum at 25°C is given below.

1. Mobility Calculation For Pure Aluminum

Aluminum is face centered cubic (4 atoms/unit cell) with a lattice parameter of 4.0496×10^{-8} cm and has 3 valence electrons per atom. So,

$$n = \frac{(4\,\text{atoms/unit cell}) \cdot (3\,\text{electrons/atom})}{4.0496 \times 10^{-8}} = 1.80695 \times 10^{23}\,\text{electrons/cm}^3,$$

and, with $\rho_{AL} = 2.6525 \times 10^{-6}\,(\Omega \cdot \text{cm})$ at 25°C,

$$\mu_{AL} = \frac{1}{1.80695 \times 10^{23} \cdot 1.6 \times 10^{-19} \cdot 2.6525 \times 10^{-6}} = 13.04\ \text{cm}^2/(\text{V} \cdot \text{sec})$$

Comparing μ_{AL} to the mobility of pure copper calculated in a similar manner ($\mu_{CU} \approx 44.2\ \text{cm}^2/(\text{V} \cdot \text{sec})$) shows that the mobility of electrons in pure aluminum is approximately 25% as great as in copper at room temperature.

The mobility of charge carriers can also be defined by the following relation:

$$\mu = \frac{\upsilon_{avg}}{\xi},\ \text{cm}^2/(\text{V} \cdot \text{cm})\quad (\text{Eq 2.2})$$

Where $\upsilon_{avg} = (\Delta x)/(\Delta t)$ is the average drift velocity of carrier charges due to an applied bias voltage (V) across the conducting material (Figure 2.1), and ξ is the electric field defined as the voltage drop per unit length of conductor.
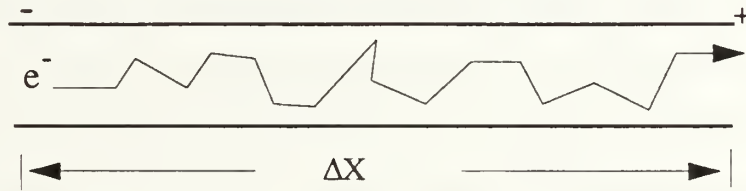

Figure 2.1 Electron Drift Schematic Diagram [Ref.. 1]

Equation 2.2 indicates that the average drift velocity is directly proportional to mobility and inversely proportional to resistivity.

B. EFFECTS OF TEMPERATURE AND LATTICE DEFECTS ON RESISTIVITY

1. Thermal Effects

The mobility of charge carriers is influenced by temperature. Figure 2.2 (a) and (b) illustrate this effect. As temperature increases, the atoms vibrate about their equilibrium positions causing of an increasingly imperfect lattice. This leads to an increase in the number of charge carrier scattering events, a decrease in drift velocity and a corresponding increase in resistivity. The thermal component of resistivity can be estimated from the following relation:

$$\rho_T = \rho_{RT}(1 + \gamma \Delta T) \quad (Eq2.3)$$

Where ρ_{RT} is the material's resistivity at room temperature, γ is the resistivity coefficient (slope of the resistivity v.s. temperature curve for a given material), and ΔT is the difference between the temperature of interest and room temperature [Ref. 1].

2. Changes Due To Lattice Defects

Lattice defects cause a significant increase in resistivity also by decreasing the charge carrier's mean free path as the number of defects increase (Figure 2.2(b),(c) and (d)). The resistivity due to lattice defects, ρ_d, i.e.,defect resistivity, is defined as the combined effect of solid solution atoms, interstitial atoms, vacancies, grain boundaries and other lattice imperfections but excluding those which are thermally induced. The combined effect of these defects is independent of temperature. During the aging process, illustrated schematically in Figure 2.3, the defect resistivity, ρ_d, decreases due to precipitation as a result of the non-equilibrium state of the initially supersaturated condition of the solution treated alloy. [Ref. 1]

3. Combined Effects of Temperature and Lattice Defects

The total resistivity due to the combined effects of temperature and lattice defects is given by the relation:

$$\rho_{Total} = \rho_T + \rho_d \quad (Eq2.4)$$

The focus of this work was to obtain a measurement of the change in the aging alloy's resistivity as a function of the change in defect resistivity, ρ_d, only, since changes in defect resistivity, ρ_d, are indicative of the aging process in aluminum alloys. The schematics in Figure 2.2 (c) and (d) correspond to the initial supersaturated condition and the precipitation (aging) process, respectively. The supersaturated condition exhibits the greatest resistivity due the small charge carrier mean free path. Due to the non-equilibrium nature of the supersaturated state, the precipitation process occurs leading to a greater charge carrier mean free path and hence lower resistivity. The effect of changes in thermal resistivity (ρ_T) during testing were minimized by subjecting a reference probe and reference sample to the same isothermal furnace environment used for aging the alloy sample.
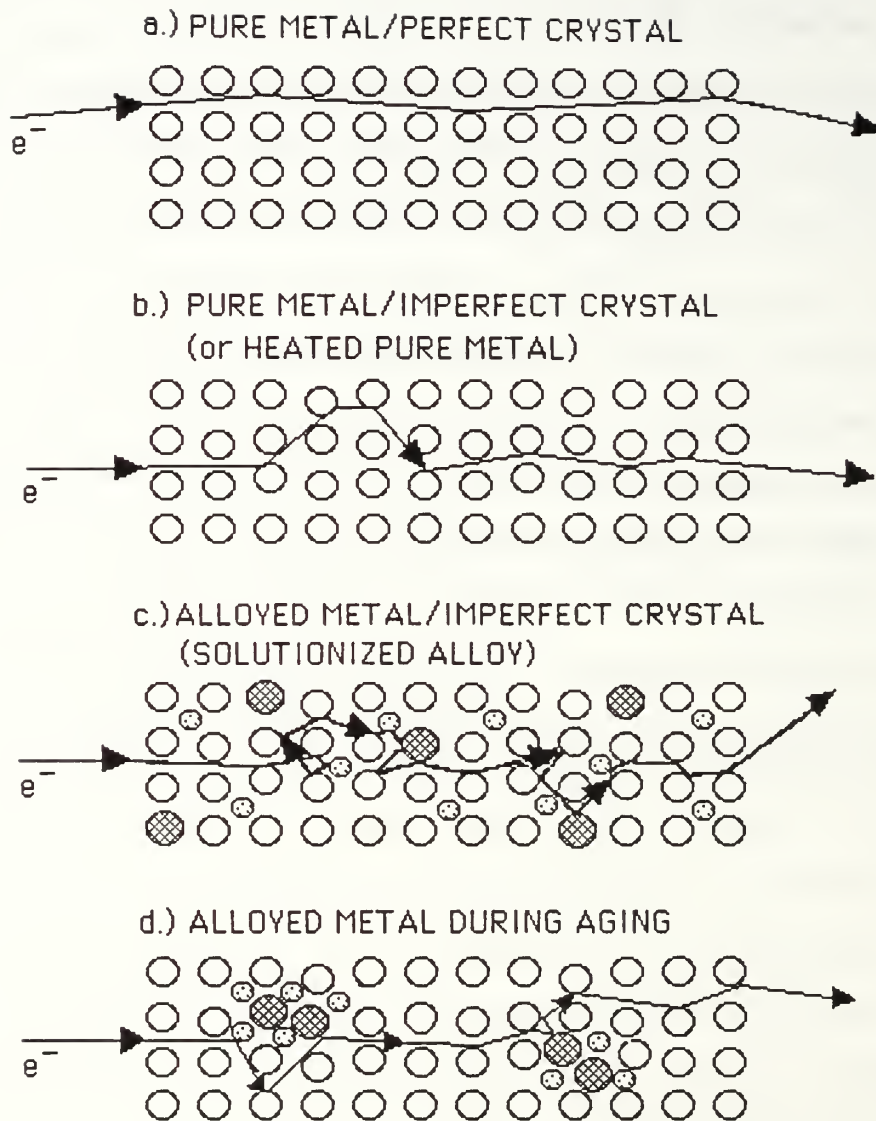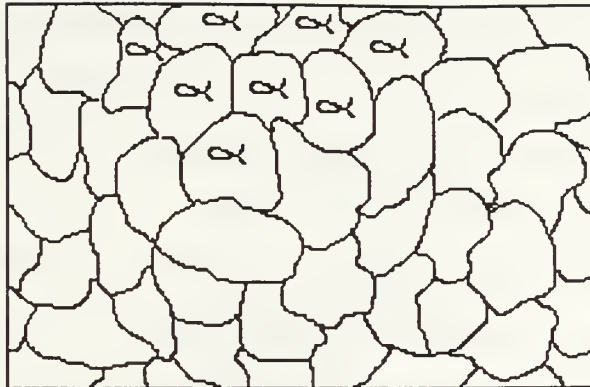
a.) PURE METAL/PERFECT CRYSTAL

b.) PURE METAL/IMPERFECT CRYSTAL
(or HEATED PURE METAL)

c.)ALLOYED METAL/IMPERFECT CRYSTAL
(SOLUTIONIZED ALLOY)

d.) ALLOYED METAL DURING AGING

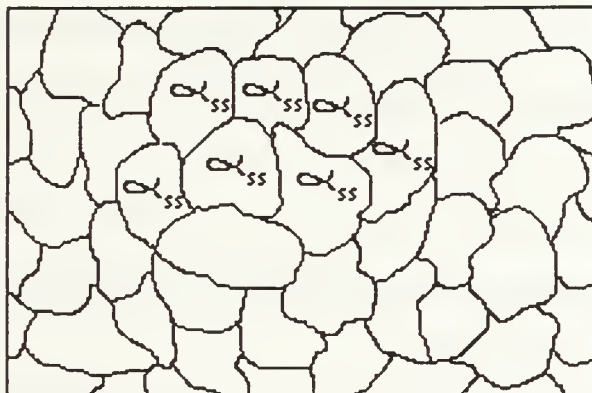**Figure 2.2 Simplified Resistivity Models**

8

a)

Equilibrium α
at temperature
above solvus
line.

b)

Supersaturated
α_{ss} after rapid
quench to room
temperature.
Large quantity
of nucleation
sites generated.
   (Unstable)

c)

Very fine ß
precipitation
particles forming
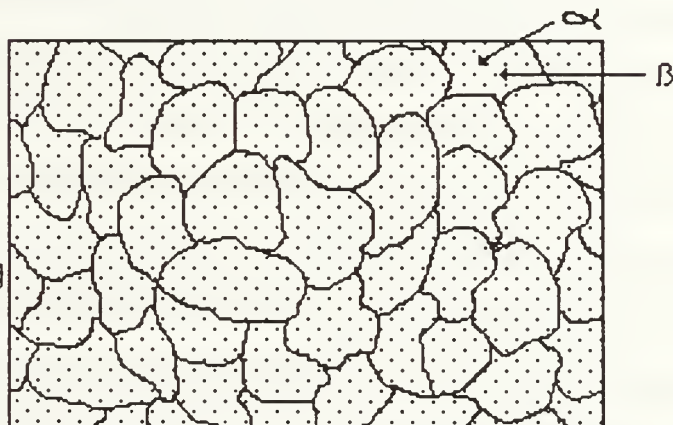at nucleation
sites during aging
process.

Figure 2.3 Simplified Aging Process Models

9

C. EDDY CURRENT PROBE THEORY

Eddy current techniques have been employed industrially for many purposes including resistivity measurements. Detailed descriptions of eddy current probe theory and/or various application techniques are developed in references 1 through 6. Therefore, this discussion is limited to the background information necessary to understand the application of eddy current techniques to monitor the isothermal aging process for age hardenable aluminum alloys.

The alloy's resistivity and magnetic permeability are the primary variables exploited by eddy current techniques when testing samples of sufficient dimensions to avoid edge effects and thickness variation effects [Ref. 2 and 6]. Age hardenable aluminum alloys are paramagnetic and have magnetic permeabilities very close to 1.0. Therefore, variation of the tested alloy's resistivity (due to changes in lattice defects during aging) is the variable exploited in this work. Changes in lattice defects correspond to changes in mechanical properties. Hence, monitoring the resistivity changes can provide an indicator of the changing mechanical properties of the material [Ref. 3 through 6].

Eddy current probes are typically driven with an alternating current source in the frequency range of 50 to 500 KHz which corresponds to penetration depths of ≈ 0.05 to 0.015 inches [Ref. 2]. This results in an alternating electric field surrounding the probe coil (Figure 2.4). When the alternating electric field surrounding the probe coil is placed near an electrically conductive sample, currents are induced within the material which are opposite in polarity to the current flowing within the coil wires. The induced eddy currents cause a back electromotive force (Emf) on the coil which increases its impedance. The level of eddy currents induced is governed by the resistivity of the tested sample. As the resistivity of the sample decreases, the level of induced eddy current increases which corresponds to an increase in the back Emf

and increased probe coil impedance. When the probes are placed appropriately as elements in an impedance bridge network (discussed in Chapter III), very small changes in impedance can be sensed as a changes in the bridge unbalance voltage (bridge output) and thus allow the aging process to be monitored.
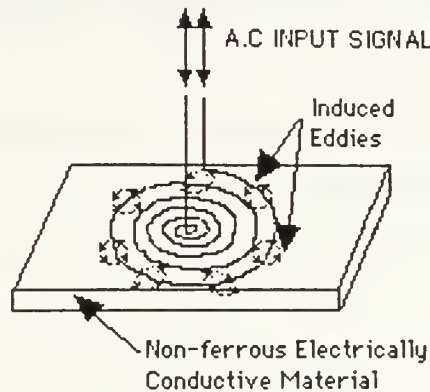

Figure 2.4 Eddy Current Probe Coil Schematic Diagram

III. EXPERIMENTAL PROCESS, PROCEDURES AND COMPONENT DESIGN

A. PROCESS/PROCEDURES OVERVIEW

The design objective for the monitoring system was to obtain a signal in real time indicative of the extent of the aging process in an age-hardenable aluminum alloy using the eddy current methods outlined in the previous chapter. The standard processing procedures for age-hardening aluminum alloys consist of solutionizing the material at an appropriate temperature for a specified length of time, rapid quenching to room temperature, and reheating at a specified intermediate temperature for a predetermined length of time in order to obtain the desired mechanical properties. The testing procedures utilized incorporated the above processing procedures with additional features to allow for the continuous measurement of the aging process. Figure 3.1 illustrates the heat treatment steps and additional procedures required by the monitoring system. The step-by-step procedures used during the experimental testing are outlined below. The bridge nulling process was accomplished prior to testing of the alloy by placing pure aluminum samples under both probes with the testing apparatus in the furnace and equilibrated at 100°C. The minimum bridge output (null) was obtained by adjusting the potentiometer.

1) Al 7075 tensile samples were solutionized at approximately 480°C for 50 minutes.
2) Samples were quickly quenched in a large water bath at approximately 25°C.
3) All Samples were immediately placed in cold storage at approximately -15°C to inhibit aging at room temperature.
4) The convection furnace was set at the desired aging temperature with the testing apparatus inside and pure aluminum test samples under each probe.
5) With isothermal furnace conditions verified and all system component settings and circuit connections verified, the data acquisition program was given the desired instructions regarding timing of sampling intervals for measuring the bridge unbalance voltage (output voltage).

6) A sample was removed from cold storage and allowed to heat until moisture could be removed from sample.

7) Upon opening the furnace, the probe bar was lifted using the lifting cam, the pure aluminum sample was removed and the alloy sample inserted under the testing probe (right probe). The probe bar was lowered allowing the probes to rest on the samples, and the furnace was closed.(This step was performed as quickly as possible to minimize heat loss.)

8) The data acquisition program was started, generating time and mV data files based on instructions given in step 5.

B.   COMPONENT FUNCTIONS

The major monitoring system components and their respective functions are given below.

1.   Testing Apparatus

The testing apparatus was required to provide for consistent sample and probe positioning as well as sufficient thermal mass to minimize temperature drop due to the insertion of the cool test sample. In order to minimize the possibility of relative movement between the sample and probes, a base plate thermal expansion coefficient similar to that of the primary alloys to be tested was required. The testing apparatus design also allowed reference samples to be easily removed to permit comparative tests with any desired reference material.

2.   Probes

The probes provided a means to induce eddy currents into reference and test samples as well as act as two elements of the impedance bridge circuit. Additionally, the footprint of the probe was minimized to avoid thermal shielding of the monitored location on the tested samples which may cause a localized retardation of the aging process.
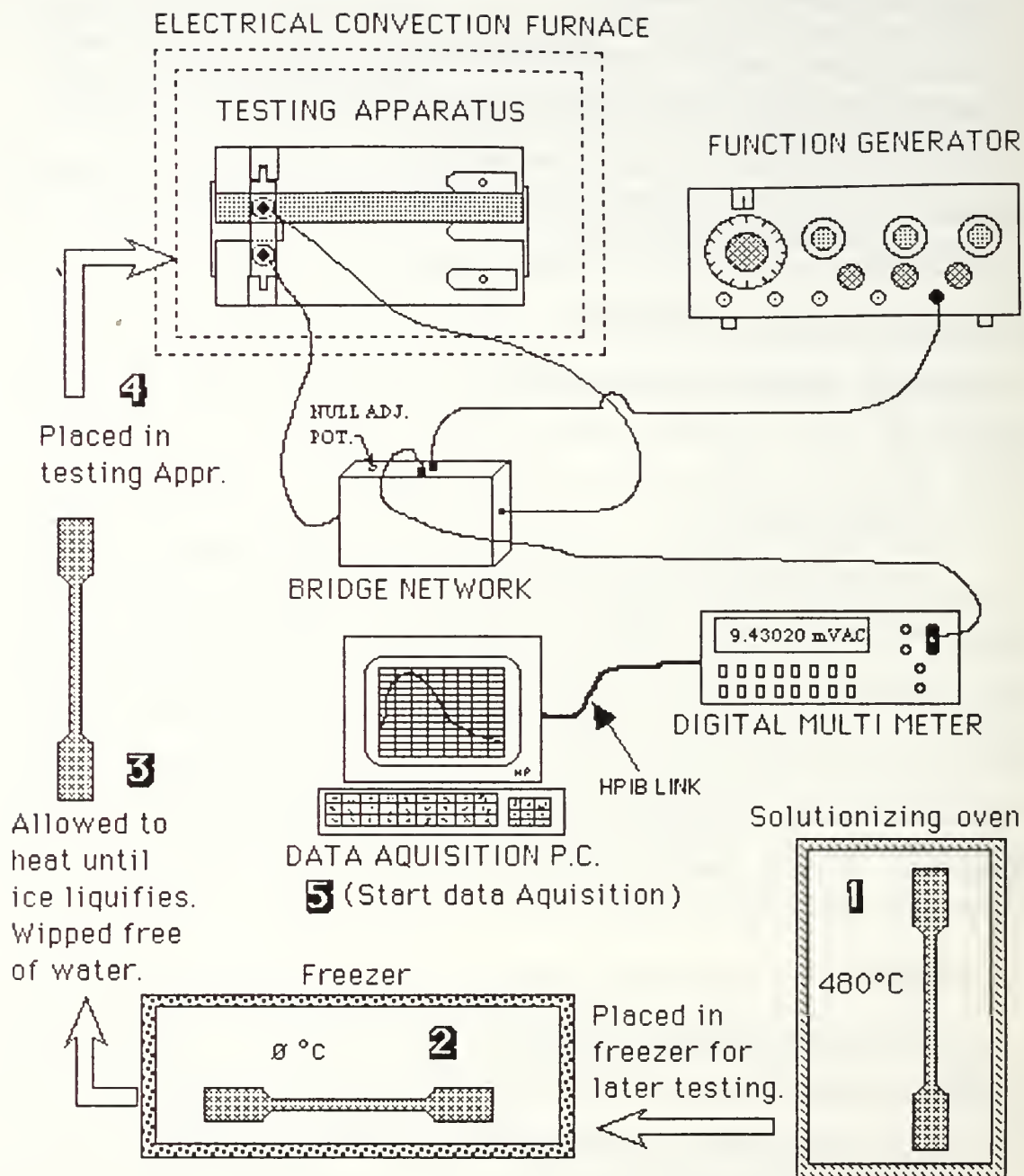
13

Figure 3.1 Testing System and Processing Schematic Diagram

14

3. Impedance Bridge Circuit

The impedance bridge network was required to provide a sufficiently sensitive means to detect resistivity changes within the test samples. Additionally, it was configured to provide a means for adjusting bridge element values to achieve an acceptable minimum initial unbalance voltage (null) with a pure aluminum test sample.

4. Function Generator

The function generator provided a stable alternating current input signal to bridge circuit. Settings used for most of the testing were: Voltage $\approx$ 10 volts (peak to peak), frequency $\approx$ 52 KHz.

5. Digital Multimeter (D.M.M.)

The D.M.M. provided a means to accurately and continuously measure the bridge unbalance voltage as well as provide a computer interface for computer sampling of measured voltage.

6. Data Acquisition Personal Computer (D.A.P.C.)

The D.A.P.C. was used to receive and store bridge unbalance voltage data from D.M.M. at specified intervals Also, it was programmed to generate a time data file corresponding to the voltage sampling intervals discussed above.

C. TESTING APPARATUS DESIGN

The testing apparatus was designed to allow the verification of the monitoring concept. Numerous equally simple, application-specific designs could be developed for industrial or other uses.
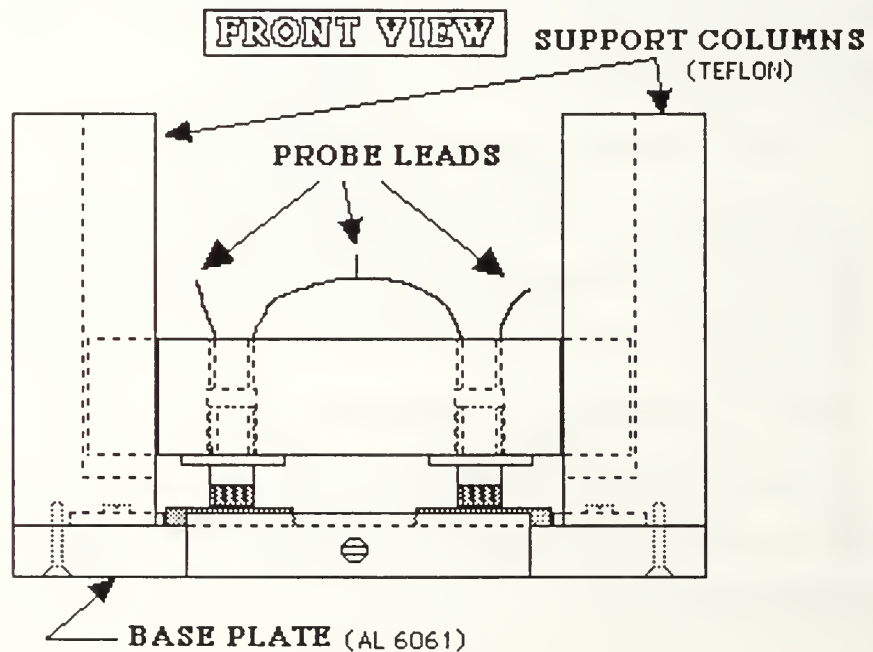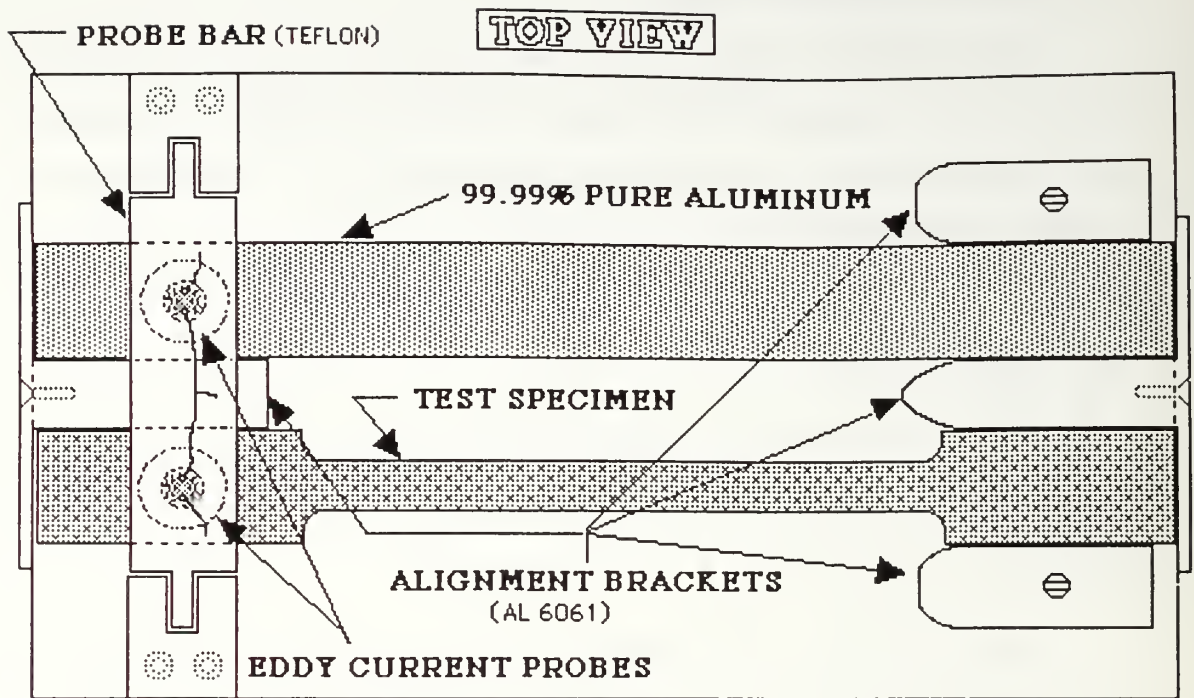
Figure 3.2 Testing Apparatus Schematic Diagram

1. General Design Considerations

Figure 3.2 illustrates the basic attributes of the final design which incorporated a balance of the design considerations listed below.

1) Simple to operate with a minimum number of moving parts
2) Maximum utilization of available materials
3) Allow for testing to be accomplished on 0.125" thick tensile bar samples of 1.0" x 8.0" overall dimensions
4) Provide sufficient thermal mass and contact area to rapidly bring cool test sample to near the desired aging temperature
5) Provide for easy and consistent placement of probes on the reference and tested samples
6) Provide constant / consistent probe-to-sample contact force
7) Minimizes amount of ferromagnetic materials used and maximize the displacement of these materials from the probe

2. Probe Design Attributes/Construction

Figure 3.3 illustrates the basic attributes of the probe design. The relevant dimensional attributes are listed below.

1) Coil slot outside Diameter - 1.0 cm
2) Collar diameter - 2.5 cm
2) Coil slot inner core diameter - 0.2 cm
3) Wire -160 turns of AWG 32 high temperature coated copper wire
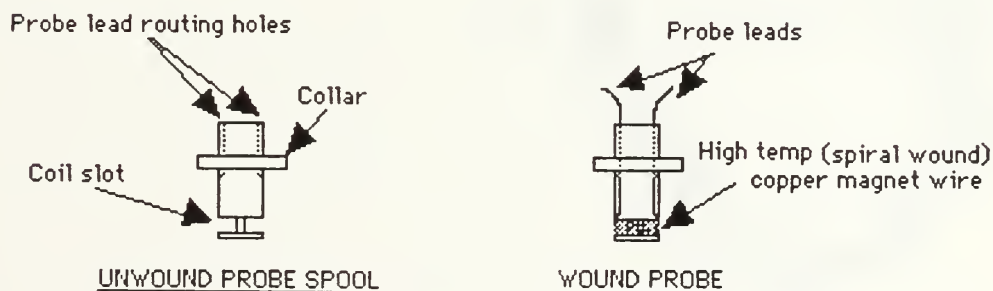4) Thickness of probe section below coil - $\approx$ 0.05 cm

Figure 3.3 Eddy Current Probe Schematic Diagram

The spools were machined from 2.5 cm Teflon ® round stock. The coil slot was cut leaving an approximately 0.2cm waffer below the slot.. The two small holes were drilled longitudinally in the spool to allow easy probe lead routing. The spools were spiral-wound with magnet wire and carefully wrapped with Teflon® tape. The waffer below the coil was then very carefully sanded to the final thickness being careful to achieve uniform thickness of the waffer.

3. Testing Apparatus Design Overview

A photograph of the testing apparatus is shown in Figure 3.3. The probe bar lifting cam (the white object at top center of photo.) is also shown in Figure 3.3. The lifting cam was inserted between the base plate and probe bar raising the probe bar assembly approximately one inch to allow sample insertion or removal. The final design's relevant dimensional attributes are listed below.

1) Base Plate(6061Aluminum)-(length x width x thickness) 8.0" x 5.0" x 0.375"
2) Support Columns(Teflon®)- 3.5"(height) x 1.0" (length and width) with 0.025" x 0.5 x 3.75" Milled slot
3) Probes (Teflon®)- 1.0 cm (diameter)
4) Probe Bar (Teflon®)- 1.0" square stock with probes mounted 0.75" from center of probe bar (longitudinally). Tongues milled to allow 0.010" clearance at all surfaces adjacent to support columns
5) Alignment Brackets(6061 Aluminum)- 0.5" (nominal) width x 0.094" thickness
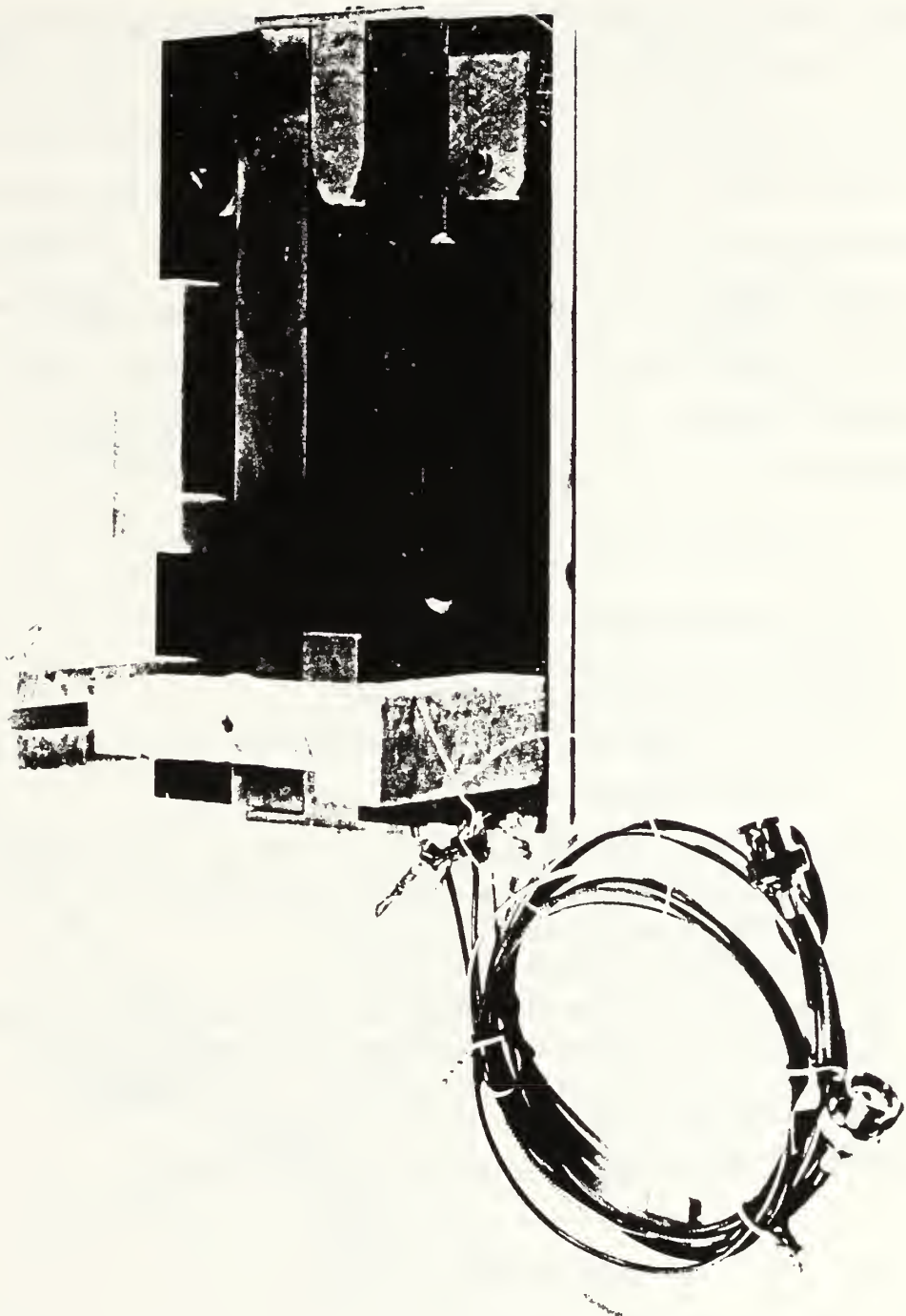6) Fasteners- Solid brass of various sizes

Figure 3.4 Photograph of Testing Apparatus and Lifting Cam

D. BRIDGE CIRCUIT DESIGN/ANALYSIS

The bridge circuit used (Figure 3.4(a))was designed and assembled based on the 50Ω nominal load requirement of the function generator, the probe impedances and the availability of other required circuit elements. A bridge circuit analysis (developed below) was conducted using the simplified bridge circuit model shown in Figure 3.4(b). The focus of this analysis was to establish the relationship between the change in testing probe (right probe) impedance, as a result of temperature deviation and/or the test sample resistivity changes during the aging process, and the resulting bridge output response. Several assumptions were made to simplify the analysis, and also, the relationships obtained were used only for qualitative comparison to the actual testing plots obtained.
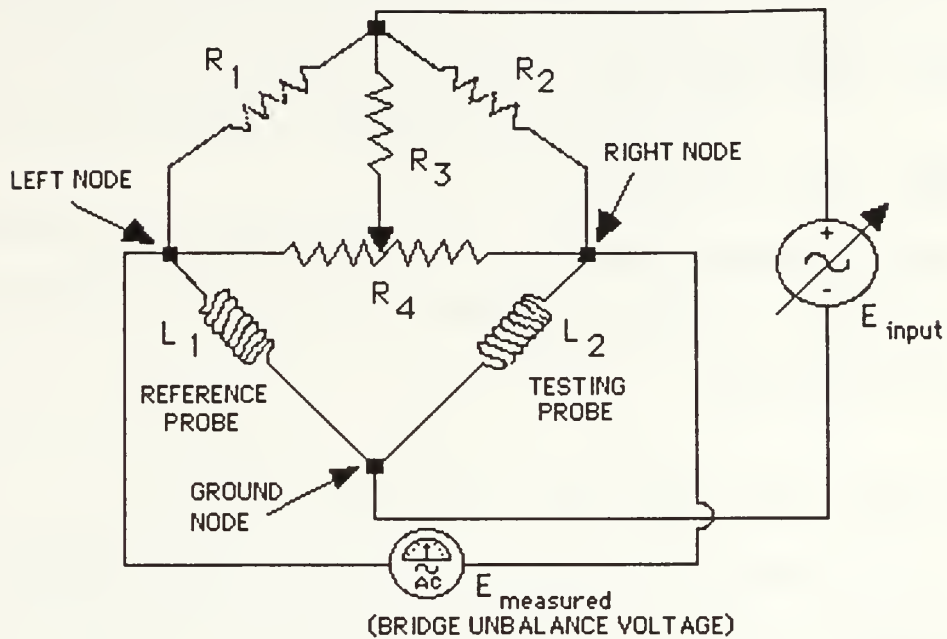
1. Circuit Analysis Assumptions

1) Mutual inductance $\approx$ zero
2) Reference probe impedance $\approx$ constant
3) Digital multimeter impedance $\approx$ infinity
4) Input peak voltage and frequency $\approx$ constant

2. Circuit Analysis

Referring to Figure 3.4(b) the following definitions were established:
1) Vi = Voltage magnitude across bridge input nodes
2) Va = Voltage magnitude at the left node
3) Vb = Voltage magnitude at the right node
4) Vo = The absolute value of the voltage difference between Va and Vb
5) Z1 = Magnitude of the total impedance of the reference probe
6) Z2 = Magnitude of the total impedance of the testing probe
7) RL = The resistance of the upper left bridge leg
8) RR = The resistance of the upper right bridge leg

20

(a) TESTING CIRCUIT SCHEMATIC DIAGRAM
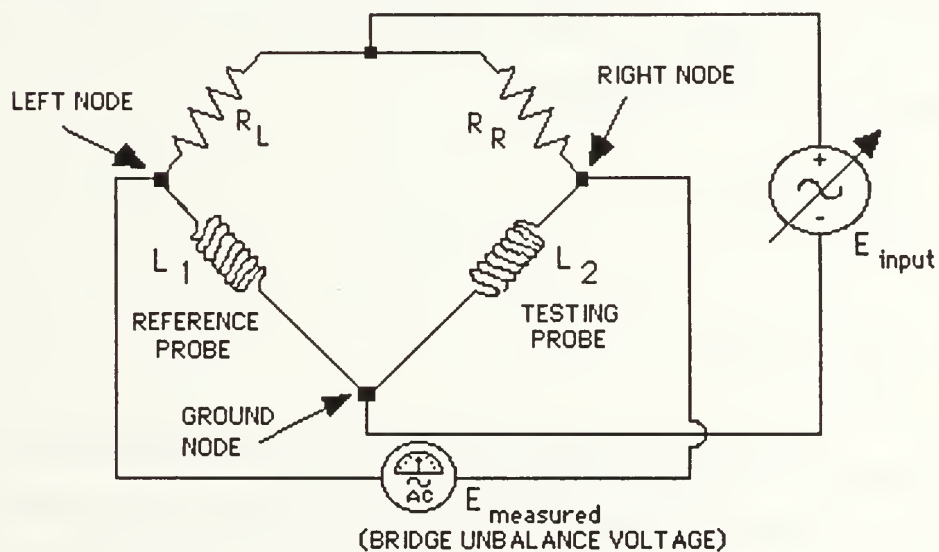

(b) (SIMPLIFIED MODEL OF CIRCUIT (a) ABOVE)

Figure 3.5 Bridge Circuit Schematic Diagrams

Using the voltage divider rule at the left and right nodes yields the following relations:

Left node -- $\quad Va = \dfrac{Z1}{(RL + Z1)} \cdot Vi \quad$ (Eq 3.1)

Right node -- $\quad Vb = \dfrac{Z2}{(RR + Z2)} \cdot Vi \quad$ (Eq 3.2)

The bridge output voltage, Vo, is the absolute value of the difference between Va and Vb which yields the following relationship between bridge circuit elements and bridge output:

Bridge output -- $\quad Vo = \left| \dfrac{Z1}{RL + Z1} - \dfrac{Z2}{RR + Z2} \right| \cdot Vi \quad$ (Eq 3.3)

For ideal conditions, i.e., using assumptions one through eight above and assuming perfect electrical match for the probe coils, the value of Vo should be zero at the perfect null condition regardless of the input voltage, Vi. Setting Vo = 0 and solving for the combinations of values for RL, RR, Z1 and Z2 which satisfy the resulting equation yields the following:

$$\dfrac{Z1}{Z2} = \dfrac{RL}{RR} \quad \text{(Eq 3.4)}$$

$$\dfrac{Z1}{RL} = \dfrac{Z2}{RR} \quad \text{(Eq 3.5)}$$

Equations 3.4 and 3.5 indicate that there are two possible combinations of bridge element values which would yield the null condition. Only one of these null conditions can be satisfied at any given time unless the value of all elements are exactly the same (magnitude and phase angle adjustments must be provided). In practice, attempting to achieve even one of the perfect null conditions above would

be tedious, time consuming and unnecessary to achieve the goal of this thesis work. Given that the intent of the monitoring system is to measure a relative change in the bridge output which is directly linked to the resistivity change in the aluminum alloy to be heat treated, there is no need to achieve a perfect null condition. Equations 3.3 through 3.5 were used in Chapter IV to develop a mathematical model of the bridge output response for qualitative comparison to actual test data.

IV. RESULTS AND DISCUSSION

A. MONITORING SYSTEM DESIGN AND OPERATION

The eddy current monitoring system was easy to operate and experienced no mechanical difficulties during more than 150 testing cycles with the exception of significant thermally induced cracks in the probe bar and support columns. The probe bar, support columns and probe spools were all thought to be made of Teflon® stock. However, it became apparent that this was not the case as the probe spools exhibited no degradation during testing.

The bridge circuit was easy to hook up and adjust to the minimum null condition. No probe balancing potentiometer was installed and hence the minimum null voltage was governed by how closely the two probes were electrically matched. The Hewlett Packard multimeter, although self-calibrating, had a 3.502 mV constant offset error which had to be subtracted from all mV data obtained in order to reflect the true output (r.m.s.) voltage. Two soldered electrical connections at the probe lead /coaxial cable junctions failed and had to be repaired at approximately 95 cycles. The 50/50 lead tin solider was heavily oxidized and very brittle, requiring re-stripping of the probe leads and coaxial cables. The newly soldered connections were wrapped with woven fiberglass sheet material in an attempt to retard further environmental degradation. Although wrapping the connections with Teflon® tape would have given better protection the fiber glass sheet provided sufficient shielding to conduct the remaining test runs.

B. BRIDGE CIRCUIT RESPONSE

The bridge output voltage (Vo) was shown in Chapter III to be given by the relation:

Bridge output -- $V_O = \left| \dfrac{Z1}{RL + Z1} - \dfrac{Z2}{RR + Z2} \right| \cdot V_i$ (Eq 4.1)

Where Z1 is the magnitude of the reference probe impedance, RL is the resistance of the upper left bridge leg, Z2 is the magnitude of the testing probe impedance, and RR is the resistance of the upper right bridge leg. The bridge analysis for ideal conditions was developed in Chapter III and resulted in the following bridge element parameter combinations for a perfect null condition:

$$\frac{Z1}{Z2} = \frac{RL}{RR} \quad \text{(Eq 4.4)}$$

$$\frac{Z1}{RL} = \frac{Z2}{RR} \quad \text{(Eq 4.5)}$$

As discussed in Chapter III, the perfect null conditions were not obtained nor were they necessary to the success of this monitoring concept. However, the null unbalance voltage should be minimized within reasonable constraints. An additional probe balancing potentiometer could easily be employed to further minimize the null unbalance voltage and is discussed in Chapter V. With only resistance adjustment incorporated into the design of the bridge circuit, minimum null condition bridge outputs on the order of 4.5 to 5.5 mV were achieved with a ten volt (peak to peak) input signal. These minimum null bridge output values were later shown to be sufficient for verification of the monitoring concept. Although the bridge circuit used was not ideal, a mathematical model of the theoretical bridge output as a function of the change in the impedance of the testing probe was used for qualitative comparison with the actual bridge output during testing using a pure aluminum test sample. The actual values of the bridge elements contained in Equation 4.3 were measured at isothermal conditions for temperatures of either 120°C or 200°C with a pure aluminum test sample using an impedance analyzer

25

which generated a one volt (peak to peak) input voltage at 50 K Hertz. The resulting values are listed in Table 4.1

TABLE 4.1 Measured Bridge Element Values

Temp.°C	RL (Ω)	RR (Ω)	Z1 (Ω)	Z2 (Ω)
120 °	84.343	82.624	20.427	19.937
200°	84.343	82.624	21.054	20.447

Based on known physical principles, i.e. a linear decrease in the resistivity of aluminum with decreasing temperature, theoretical bridge output v.s. time curves were calculated and plotted as shown in Figure 4.1.
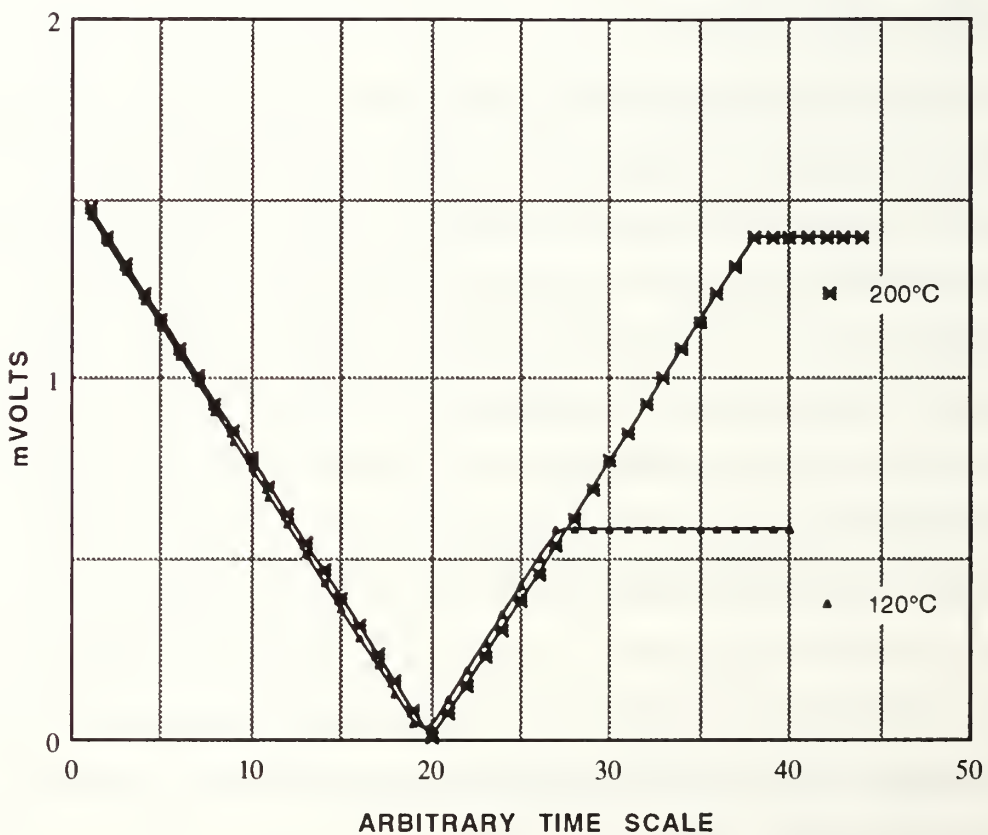

Figure 4.1 Theoretical Bridge Output Response (Pure Aluminum Samples)

In practice, this involved assumption of initial values for Z2 (testing probe impedances) which were higher values than shown in Table 4.1. These values were decreased in steps to the final values shown in Table 4.1. The higher starting values of Z2 reflect a lower resistivity of the cool test sample when initially inserted into the testing apparatus. The curve characteristics shown in Figure 4.1 were then compared to the plots obtained for actual testing with the pure aluminum samples and shown in Figure 4.2. The response is clearly very similar to the predicted bridge output. Also, the fully annealed pure aluminum does not exhibit any change in resistivity under isothermal conditions. The constant final steady-state output indicated that the testing system's response under isothermal conditions is consistent with the absence of aging response under these conditions.
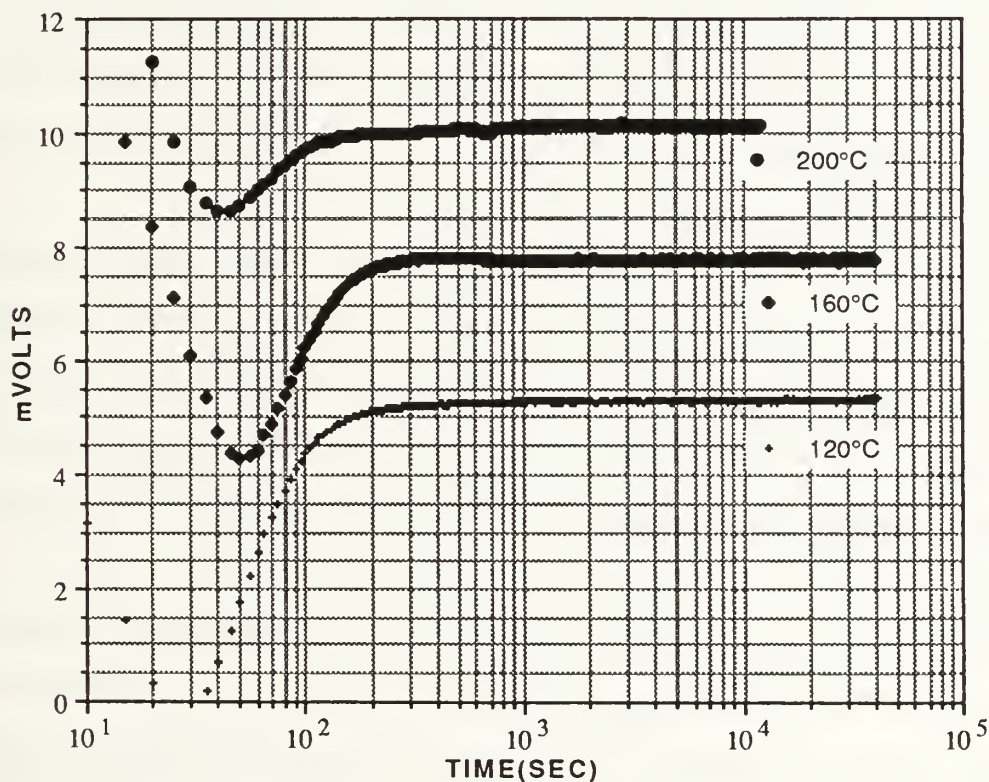

Figure 4.2 Experimental Bridge Output Response (Pure Aluminum Samples)

C. EXPERIMENTAL MEASUREMENT RESULTS FOR Al 7075 ALLOY

The mV vs. time curves in Figure 4.3 illustrate the bridge output response characteristics as ANSI 7075 aluminum samples were aged for various times and temperatures. The bridge output response characteristics for the temperature transient region were very similar to those obtained from the pure aluminum samples (Figure 4.2). The peak bridge output values correspond to the point at which the test samples reach thermal equilibrium. A characteristic and continuous decrease in bridge output after reaching thermal equilibrium was seen for all test conditions and the rate of decrease was temperature dependent. The resistivity of the 7075 alloy is expected to be greatest in the solutionized state, and hence the bridge unbalance condition would be at its maximum (under isothermal conditions) due to the testing probe impedance being at its lowest value. Correspondingly, a decrease in the bridge output from this maximum point reflects a decrease in the alloy's resistivity with aging. Furthermore, the greater rate of decrease in the alloy's resistivity with increasing aging temperature is consistent with the physical metallurgy of age hardening in aluminum alloys.

The peak bridge output values decreased with increasing aging temperature where as where the corresponding value increased with temperature for the pure aluminum sample test runs (Figure 4.2). This reversal in peak output voltage trend with temperature is a result of the differences in the relative magnitudes of the testing probe impedances when testing the alloy samples as opposed to testing the pure aluminum.

The question of repeatability of system output was addressed by conducting multiple tests of 7075 alloy samples at the same aging temperature and initial bridge null settings. Figure 4.4 illustrates a typical result of these tests. Slight deviations in the peak bridge output voltages were noted.
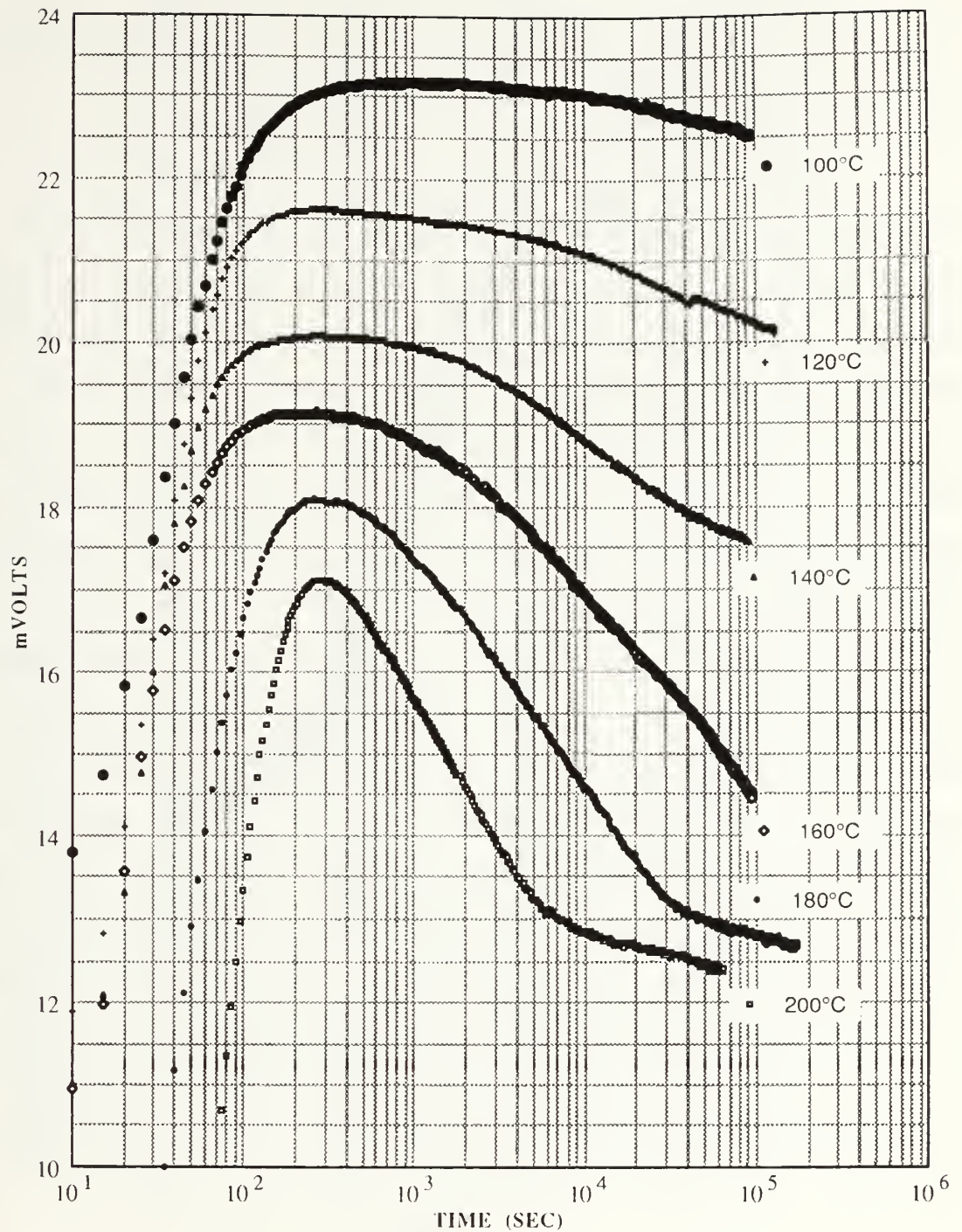
Figure 4.3 Experimental Bridge Output Response for AL 7075 Aged at Various Temperatures
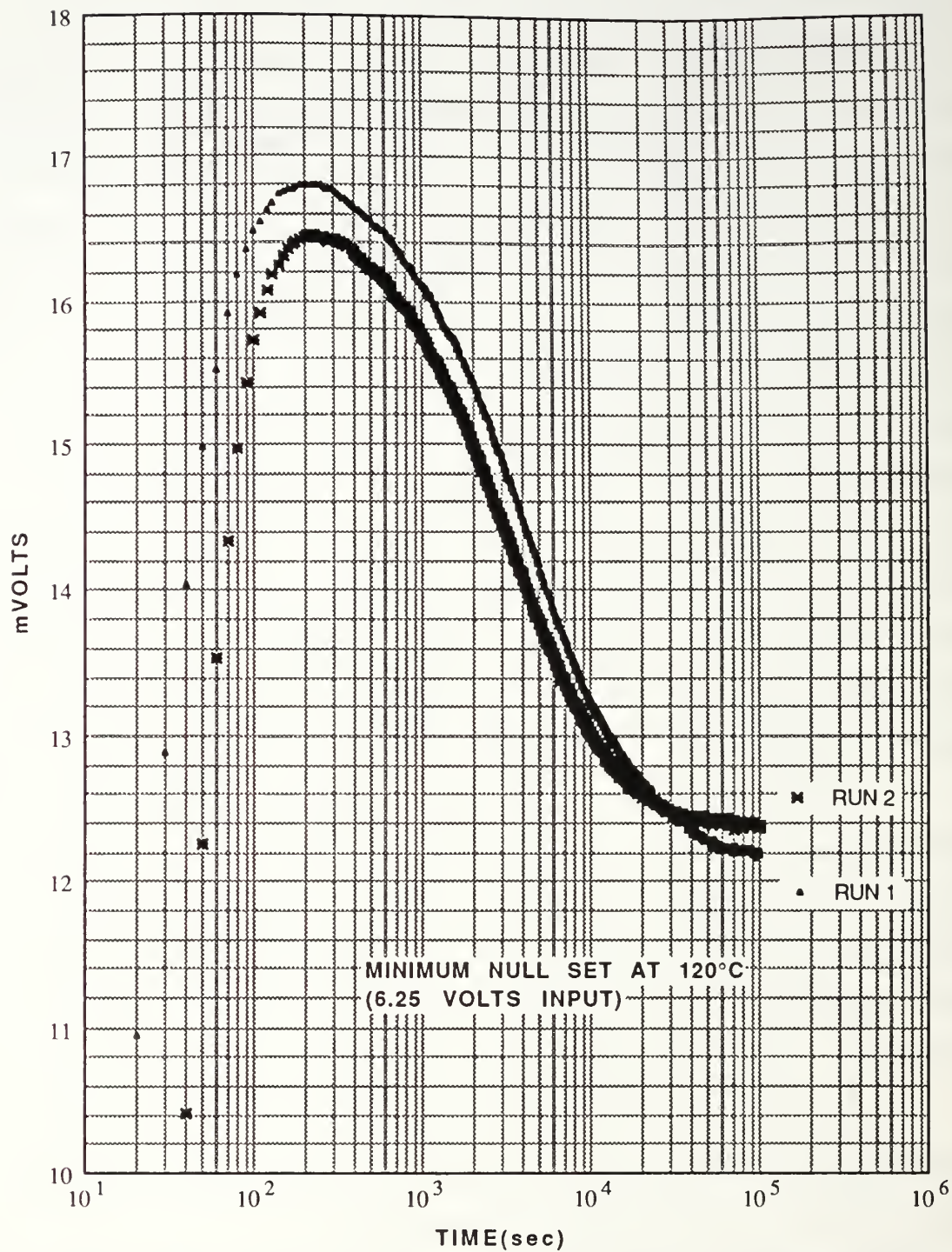
29

Figure 4.4 Experimental Bridge Output Response for Two Test Runs With AL 7075
Aged at 200°C

The differences are the result of the extreme sensitivity to variations in mechanical displacement from the test sample (lift-off distance) as well as sample surface irregularities. Any type of slight scale or foreign matter would also cause such variations. Although attempts were made to minimize these factors in this work, they would be present if such a system is applied to industrial use.

The small test-to-test variation in output voltages could easily cause the testing system to be inadequate for precise monitoring of the aging process. However, these effects were minimized by a simple signal processing scheme. The signal processing scheme consisted of calculating a mean peak bridge output voltage over a short time span (30-60 sec.) as the sample approached thermal equilibrium. Computing the percent deviation from these mean peak voltage values resulted in percentage deviation data which were very consistent and more indicative of resistivity changes within the test samples. Application of this signal processing scheme to the data plotted in Figure 4.4 is shown in Figure 4.5. The signal processing scheme did not change the characteristics of the bridge output, but merely nullified the adverse effects of minor mechanical irregularities at the probe/test sample interface. Figure 4.6 is a percent deviation v.s. time plot of the data from Figure 4.3 and indicative of the final monitoring system output for various aging temperatures. Correlation of these aging curves to the resulting mechanical properties is needed to ensure that consistent mechanical properties are obtained when the aging process is stopped at any given value of percent deviation for a specified aging temperature.
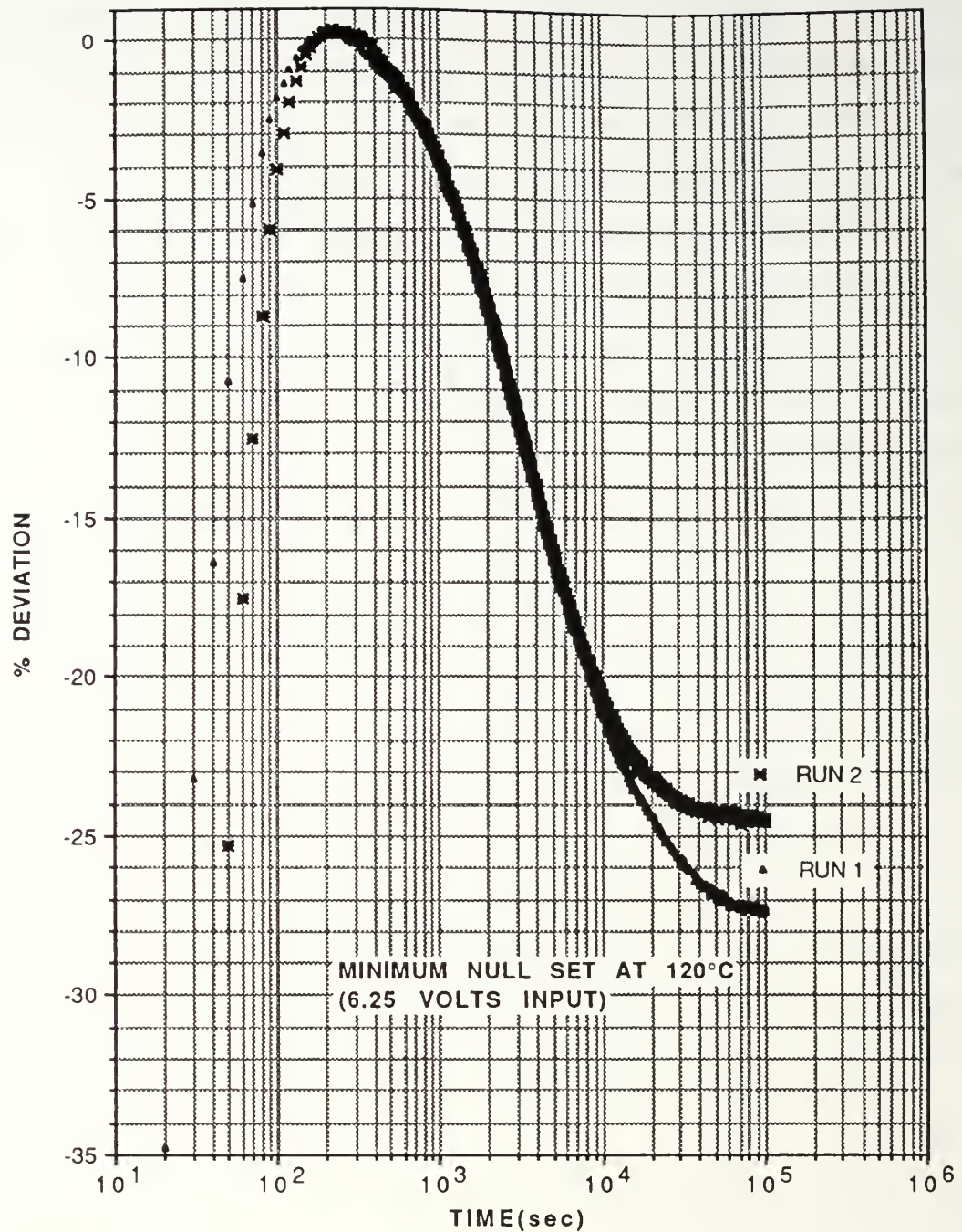
Figure 4.5 Plot of Data From Figure 4.4 After Applying Signal Processing Scheme to Yield Percent Deviation
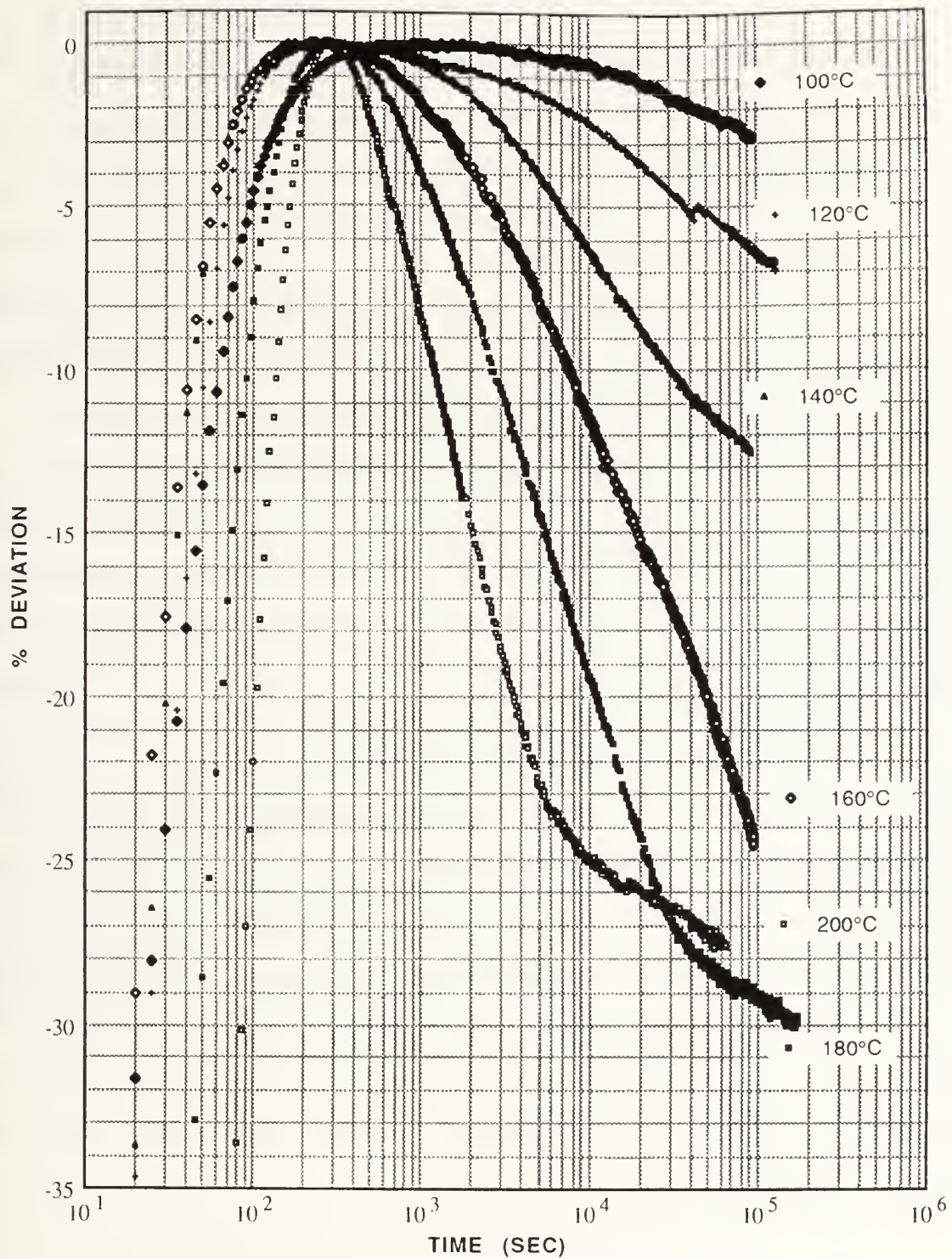
Figure 4.6 Plot of Monitoring System Final Output From Data Plotted in Figure 4.3

33

V. CONCLUSIONS AND RECOMMENDATIONS

The conclusions and recommendations discussed below were drawn as a result of this thesis project.

A.   CONCLUSIONS

1.   Testing Apparatus Design

The functional aspects of the testing apparatus were sound and need not be altered to perform future testing. However, a new probe bar and support columns need to be manufactured from Teflon® stock suitable for 200°C service.

The one-centimeter diameter probes appeared to be mechanically sound showing no indications of material or electrical degradation after more than 150 cycles. The probes also provided detectable impedance changes as a result of the aging process. However, no other probe sizes were tested to determine the optimum probe coil configuration.

2.   Bridge Circuit Design and Operation

The bridge circuit was easy to adjust for minimum null and provided for easy connection to the appropriate components of the monitoring system. Sufficient sensitivity was achieved with final output percent deviations on the order of 6-7% after approximately 24 hours of aging at 120°C (approximately T6 aging condition).

The bridge circuit allowed only for balancing the resistance legs of the bridge circuit and resulted in a minimum null condition which could be improved by installing a balancing potentiometer between the probe coils (see recommendations).

3. Monitoring Concept

The monitoring concept was determined to be valid as verified by the resulting significant decreases in percent deviation from the mean peak bridge output voltages with time at isothermal conditions. Also, the rate of decrease in final output increased with aging temperature which is consistent with the known aging response of AL 7075.

B. RECOMMENDATIONS

The bridge circuit design should be revised to allow independent balancing of the probe impedances (magnitudes). Figure 5.1 shows a simple alternate circuit which would provide the necessary additional adjustment.

Mechanical testing of aluminum alloy samples aged to the same percent deviation needs to be conducted to establish and verify the direct link between the testing system output and the corresponding mechanical properties. Conducting multiple tests, as mentioned above, at various aging temperatures would result in system characteristic curves of percent deviation v.s. mechanical property.

The voltage source testing frequency of ≈ 52 KHz. was used to maximize depth of penetration. However, greater measurement sensitivity could be achieved at greater frequencies. Further tests need to be conducted to optimize the balance between test frequency and depth of penetration.[Ref. 2 and 6]
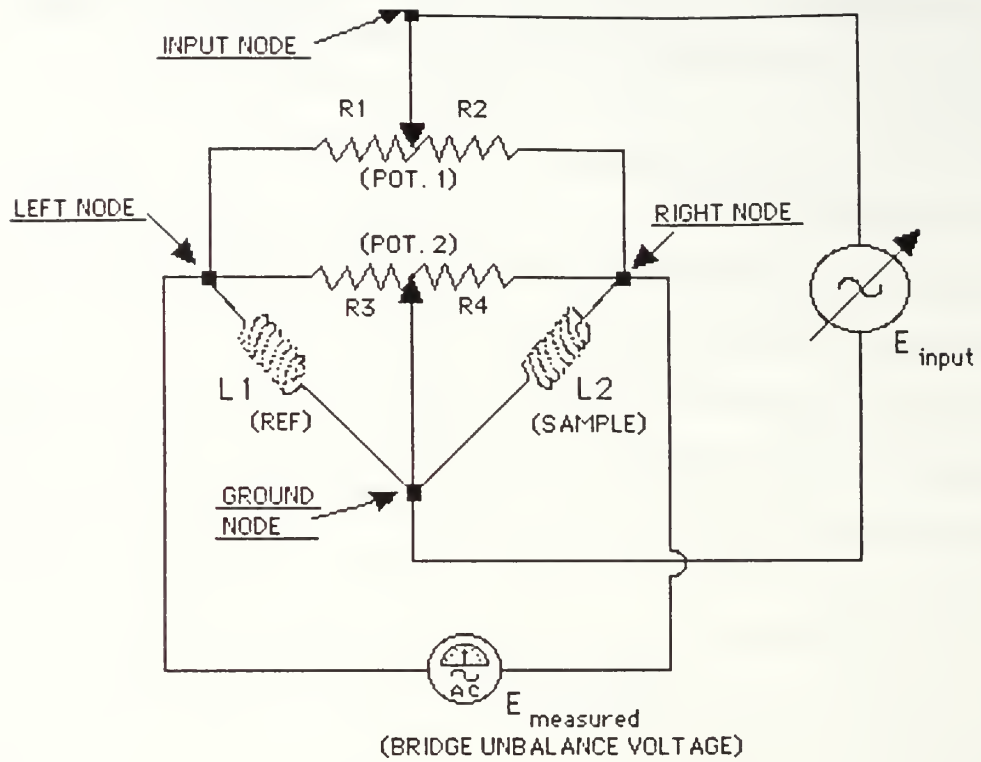
Figure 5.1 Alternate Testing Circuit Schematic Diagram

LIST OF REFERENCES

1. Askeland, Donald R., *The Science and Engineering of Materials,* PWS-KENT Publishing Co.,1989.

2. *Metals Handbook,* 9th Ed., Vol. 2, edited by Baker, Hugh, et. al., ASM International,1979.

3. *Metals Handbook,* 9th Ed., Vol. 17, edited by Lampman, Steven R., et. al., ASM International,1989.

4. Rummel, W. D., *Characterization of 2014, 2219, 6061 and 7075 Aluminum Alloy Heat Treatment Response by Eddy Current Conductivity, Hardness and Mechanical Properties,* American Society for Nondestructive Testing, Inc., 1980.

5. Seltzer, David D., *Correlation of Conductivity to Mechanical Properties of Age-Hardenable Aluminum Alloys Using Eddy Current Methods,* Paper from the "Proceedings for the Fifth International Conference on Nondestructive Testing", Dept. of Energy, Mines and Resources,1969.

6. Chihoski, R. A., et. al., *Effect of Specimen Thickness, Cladding and Lift-off Adjustment on the Conductivity of 7075-T6 Aluminum Alloy,* Paper from the "Proceedings for the 1st National Symposium for Nondestructive Testing of Aircraft Components", 1960.

INITIAL DISTRIBUTION LIST

1. Defense Technical Information Center   2
    Cameron Station
    Alexandria, VA   22304-6145

2. Library, Code 52   2
    Naval Postgraduate School
    Monterey, CA   93943-5000

3. Department Chairman, Code ME/Kk   1
    Department of Mechanical Engineering
    Naval Postgraduate School
    Monterey, CA   93943-5000

4. Dr. William Fraser, Code 6063   1
    Naval Surface Warfare Center
    Warminster, PA 18974

5. Mr. John Flairty   1
    Flare Technology
    671 Grosvener LN
    Elk Grove Village,IL 60007

6.   Lt John G. Esarey, USN   2
    Hc 64 Box 270
    Bristow, IN 47515